EURASIP Journal on Applied Signal Processing 2003:3, 276–286

Robust Clustering of Acoustic Emission Signals Using Neural Networks and Signal Subspace Projections

Vahid Emamian
Department of Electrical & Computer Engineering, University of Minnesota, 200 Union St. SE, Minneapolis, MN 55455, USA
Email: emamian@ieee.org

Mostafa Kaveh
Department of Electrical & Computer Engineering, University of Minnesota, 200 Union St. SE, Minneapolis, MN 55455, USA
Email: mos@ece.umn.edu

Ahmed H. Tewfik
Department of Electrical & Computer Engineering, University of Minnesota, 200 Union St. SE, Minneapolis, MN 55455, USA
Email: tewfik@ece.umn.edu

Zhiqiang Shi
Woodruff School of Mechanical Engineering, Georgia Institute of Technology, Atlanta, GA 30332-0405, USA
Email: ShiZ@corning.com

Laurence J. Jacobs
School of Civil & Environmental Engineering, Georgia Institute of Technology, Atlanta, GA 30332-0355, USA
Email: ljacobs@ce.gatech.edu

Jacek Jarzynski
Woodruff School of Mechanical Engineering, Georgia Institute of Technology, Atlanta, GA 30332-0405, USA
Email: jacek.jarzynski@me.gatech.edu

Received 5 July 2001 and in revised form 15 August 2002

Acoustic emission-based techniques are being used for the nondestructive inspection of mechanical systems. For reliable automatic fault monitoring related to the generation and propagation of cracks, it is important to identify the transient crack-related signals in the presence of strong time-varying noise and other interferences. A prominent difficulty is the inability to differentiate events due to crack growth from noise of various origins. This work presents a novel algorithm for automatic clustering and separation of acoustic emission (AE) events based on multiple features extracted from the experimental data. The algorithm consists of two steps. In the first step, the noise is separated from the events of interest and subsequently removed using a combination of covariance analysis, principal component analysis (PCA), and differential time delay estimates. The second step processes the remaining data using a self-organizing map (SOM) neural network, which outputs the noise and AE signals into separate neurons. To improve the efficiency of classification, the short-time Fourier transform (STFT) is applied to retain the time-frequency features of the remaining events, reducing the dimension of the data. The algorithm is verified with two sets of data, and a correct classification ratio over 95% is achieved.

Keywords and phrases: acoustic signals, classification, mechanical failure, neural networks, subspace projections, SOM, PCA, RBF.

1. INTRODUCTION

An acoustic emission (AE) signal is an ultrasonic wave emitted from the deformation of materials. Specifically, AE is the transient wave resulting from the sudden release of stored energy during a deformation and failure process, such as fretting or crack growth in a material. The AE signal conveys useful information about the fatigue behavior of a specimen, and is one of the several nondestructive inspection methods for automatic fault monitoring in mechanical systems.

The increased reliability and safety standards of engineering structures requires the detection of the precursor or onset of failures. Compared to other nondestructive testing (NDT) techniques, AE has the advantage of real-time continuous monitoring of in-service structures [1]. A major issue in applying the technique, however, is how to differentiate the events of interest, that is, those due to crack growth or imminent failure, from noise of various natures in a large dataset. Often the real AE events are measured in the presence of noise due to vibration, fretting, electromagnetic interference, and so forth, and automatic noise rejection is required before correlating AE activities with crack initiations or progressive failures. This essentially becomes a problem of pattern recognition and classification for random processes. In many cases, traditional signal processing techniques such as filtering, energy analysis, spectrum analysis, and so forth, are insufficient to separate the two as the noise often has similar temporal and frequency features as the AEs due to crack activities, and new alternatives have to be explored. One approach is to use neural networks that are capable of automatically discovering features and patterns in a larger collection of almost random observations [2, 3, 4, 5, 6].

This article presents a suite of algorithms, which together have proved effective for automatic clustering and separation of AE events based on multiple features extracted from the original test data. The procedure consists of two steps. First, the noise events are separated from the events of interest and subsequently removed, using a combination of covariance analysis, principal component analysis (PCA), and differential time delay estimates. The original data is reduced by up to 70% after this step. The second step processes the remaining data using a neural network, which clusters AE signals and noise signals to separate neuron outputs. To improve the efficiency of classification, a short-time Fourier transform (STFT) is applied to retain the time-frequency characteristics of the remaining events, and reducing the dimension of the data. The performance of the algorithm has been validated on some eight sets of experimental data involving significant levels of crack-like signals generated from the mechanisms that hold the sample. Two sets of the data were determined by inspection to have been obtained under the most reliable conditions. Hence, this paper concentrates on the presentation of the results for these two sets that have resulted in AE classification accuracies in excess of 97%. The remaining data sets resulted in accuracies in the range of 85%–95%. In an alternate approach, an AE signal subspace, that is, one formed by a set of orthogonal basis set that retains the features of AE signals, is computed from the separated AEs. When applied to data from new tests, signals of similar features, that is, AE events of the same origin, are selected automatically. The example in this study shows a correct selection ratio of 90%.

2. AE EXPERIMENTS AND DESCRIPTION OF THE DATA

2.1. Data acquisition system and transducers

A four-channel fast data acquisition system was used to continuously monitor and collect data from the AE transducers during mode-I fatigue test [7]. The system has a minimum echo delay time of 0.1 ms for recording successive events. The output from each transducer is connected to a preamplifier that is adjustable from −20 dB to 40 dB. Output from each preamplifier is then split into two in the main data acquisition unit: one to the trigger circuit and the other to the signal acquisition circuit. In each circuit, there is separate adjustable filter and gain setting. Therefore, the output signal from each of the four AE transducers is amplified, divided into a data signal and a trigger signal, as described above. A trigger level can be set separately for each of the four channels. In the present measurements, a single trigger level was set for the trigger signals from all four channels. When the amplitude of a trigger signal from anyone of the four AE transducers exceeds the preset level, the data signals from all transducers are digitized, saved, and transferred to a desktop computer. The trigger level was set to be 3 to 6 dB above the noise level of the system, which was determined as follows. The trigger level was gradually increased until the system began to capture signals continuously before the application of fatigue strains. This level was then taken as the noise level of the system, and the dominant source is assumed to be electronic noise in the preamplifier. The setting for recording the data used in this study is shown in Table 1.

Table 1: Typical setting of the AE acquisition system.

Preamplifier gain	40 dB
Signal setting	Filter: 20 kHz ∼ 4 MHz; Gain: 15 dB
Trigger setting	Filter: 100 kHz ∼ 1 MHz; Gain: 21 dB
Trigger level	0.1 v
Threshold of detection	89 μv
Sampling rate	5 MHz
Record length	1024 (in sample)

For the test samples used in the present study, the space available for the placement of AE transducers is limited. Small piezoactive ceramic elements, therefore, were assembled for use as AE sensors. The elements were 6 mm long, 2 mm wide, and 0.5 mm thick, and were poled to respond to displacements or stresses in the thickness direction. The fundamental thickness resonance was 4 MHz, well above the frequency spectrum of typical AE signals that normally extends from 50 kHz to 1 MHz. These sensors were calibrated by a laser ultrasonic technique [7].

2.2. Description of the test data

The data used in this work was collected from the mode-I fatigue test of 13-8 stainless steel. The dimensions of the specimen and the sensor locations are shown in Figure 1. The center notch introduces stress concentration that causes microcracks to initiate at the root and allows crack sizing via a long-range microscope.

The sensors are placed in positions such that transient AE signals emitted from a notch crack arrive at the four sensors at approximately the same time. If the transients are clean and well defined, spatial filtering via the time of arrival

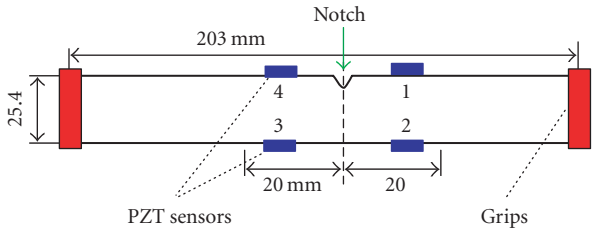

Figure 1: Specimen dimension and AE sensor locations (unit: mm).

Table 2: Summary of the tests (total events: number of events recorded by each sensor, AE events: AE signals emitted from a notch crack).

Test	Total events	AE events	Percentage of AE
1	3027	385	12.7%
2	2141	192	8.97%

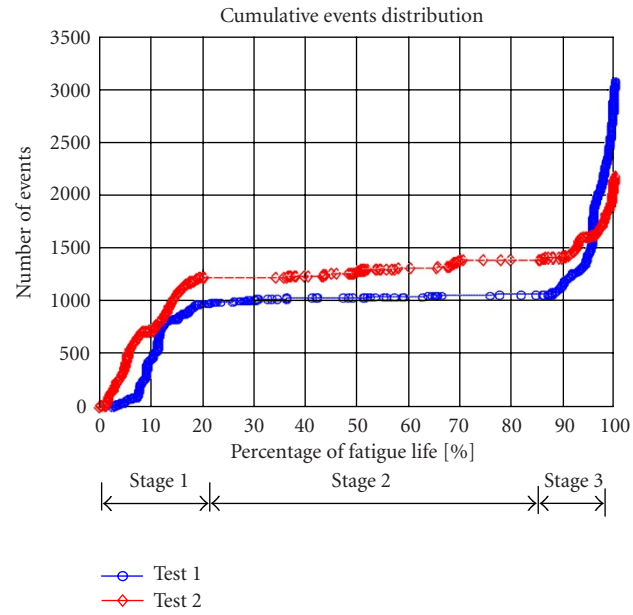

Figure 2: Event (acoustic activities) distribution during the fatigue process.

enables the elimination of grip friction noise. The specimen is fatigued on an MTS (MTS Systems Corp. makes the instrument used here) testing machine at a stress interval between 21.7 $\sim$ 217 Mpa ($r = 0.1$) at a frequency of 10 Hz. A summary of the data from two tests is given in Table 2. Here AE events have been selected manually. Each event has a length of 1024, hence data from tests 1 and 2 are 3027×1024 and 2141×1024 matrices, respectively.

Figure 2 shows the cumulative event distribution of the two tests, from which three stages are identified. The first stage is accompanied by severe activities from the start of the fatigue loading and takes approximately 20% of the fatigue. It follows by a dormant period that consists of the main portion of the fatigue life, up to almost 70%. This is denoted as stage 2. A micro-crack will be formed at the end of this stage and start to propagate at accelerated rate under the constant loading, accompanied again by severe activities. This takes about 10% of the fatigue until final fracture. Examination of the events in post-processing reveals that most AEs occur in stage 3, however, stage 1 mainly consists of grip noise. For an AE event, the produced response arrives at the four sensors almost instantaneously. While the noise event is generated at the sample end close to transducers 1 and 2, and it arrives 2.5 μs earlier at transducer 1 and 2 compared to the arrival at transducers 3 and 4. It is also noticed that AEs produced from crack growth are burst type, that is, the wave packet is short, and generally have more higher frequency contents than the grip noise.

Frequency spectra of the recorded events from various fatigue tests revealed that the signal bandwidth is mainly in the frequency range from 100 kHz to 1 MHz. Notably, AE events contain more high frequency components, that is, between 500 kHz to 1 MHz, than the noise. To increase the signal-to-noise ratio, a band-pass filter from 100 kHz to 1 MHz is applied to all the test data before further analysis.

In situations where the sources of AE and noise are spatially separated, the differential time-delay estimate is a simple, yet accurate method in differentiating the two. Using this criterion and noticing the burst feature, AEs in test 1 and test 2 are manually selected via visual inspection of the original test data. This process, however, is difficult to *automate*, as a threshold-based delay estimate has high variance for low signal-to-noise ratio events or events that are not well defined. The philosophy in achieving automatic classification, therefore, has to explore schemes that can distinguish the AE and noise in different aspects, successively reduce the noise presence, and eventually come up with a clean set of AE events.

3. FEATURE EXTRACTION OF AEs AND NOISE

The section describes multiple approaches for successively separating the AE signals from the noise in a large data set, using principal component analysis, differential time-delay estimate, covariance analysis, and space-time processing.

3.1. *Principal component analysis (PCA)*

The central theme of PCA [8] is to "reduce the dimensionality of a data set in which there are a larger number of interrelated variables, while retaining as much as possible the variation present in the data set" [9]. The reduction is achieved by transforming the original data to a new representation, the principal components, ordered such that the first few components retain most of the variation present in the original data. The original test data are high-dimensional matrices (test 1: 3027×1024; test 2: 2141×1024) and therefore requires a huge amount of computational effort. We keep the first two PCs only; hence the algorithms need less memory and run substantially faster.

One major application of PCA is to project and visualize

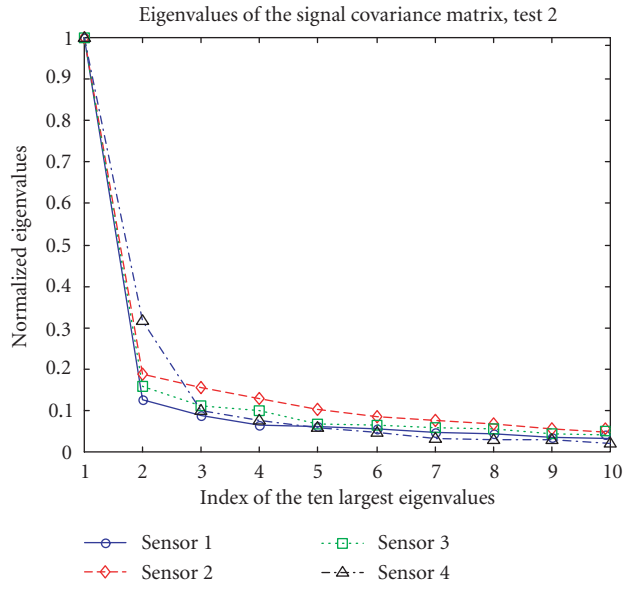

FIGURE 3: The ten largest eigenvalues of the signal covariance matrix for test 2.

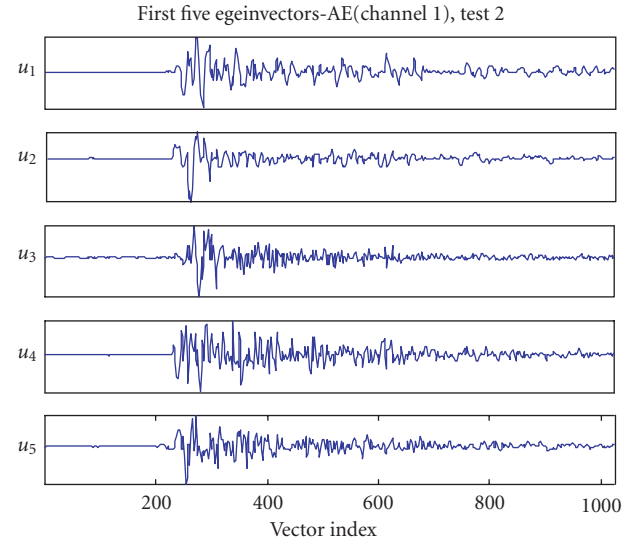

FIGURE 4: First five principal vectors for crack-generated AE signals of test 2.

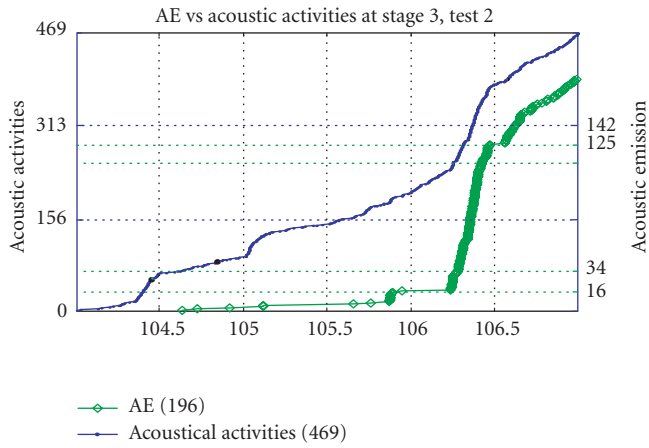

FIGURE 5: Acoustic emissions (AE) at late stage of fatigue (test 2).

the original data in the subspace of principal vectors, with the corresponding PCs being the coordinates. This is implemented for clustering AEs in this paper. To extract the features of AE signals, we first analyze the ensemble of 192 AE events from test 2. Figure 3 shows the distribution of the ten largest eigenvalues of the sample covariance matrix. It is clear that the first few principal vectors dominate the description of the ensemble, and the first few PCs are sufficient for characterizing the signal in the subspace. The large ratio of the first eigenvalue to the second and third indicates a high degree of similarity between the signals in the ensemble, that is, AEs generated from well-developed cracks are very similar, and the first principal vector describes this common feature. For illustration and graphical presentation purposes, the following analysis uses only the first two PCs, or projections of the original data onto the first two principal vectors. We could clearly use more PCs for more complete representation.

Figure 4 shows the first five eigenvectors describing the "group features" of the original AE ensemble. The corresponding PCs, computed by projecting each event to the above eigenvectors, are coordinates of each original event in the "feature" space. Notice that most of the energy is carried in the lower frequency components (first eigenvector), while the higher dimensions characterize the higher frequency details for the signal as well as the wideband noise present in the measurements.

3.2. Covariance analysis

When a fairly large crack is formed and then grows at constant rate, the generated AE events often demonstrate high degree of similarity. This is shown in Figure 5 as periods of rapid rise in the cumulative event count. One effective technique in describing the similarities of these AEs is covariance analysis or normalized maximum cross correlation between an event and adjacent events [10, 11]. Figure 6 shows the gray scale covariance matrix of AE events in the test 2. The generally banded structure of the matrix indicates significant correlation between adjacent waveforms, which coincide with the regions of rapid rise in the cumulative event count as shown in Figure 5.

Figure 7 is the overlapped plot of the high correlation waveforms, and shows an almost deterministic nature. It appears that there is the potential of using cross-correlation among succeeding events over a time window as an indicator of the changes in the development and growth stage of a crack.

3.3. Features of noise

One source of noise in AE testing is mechanical vibrations. This noise, in general, has low frequency content and can be

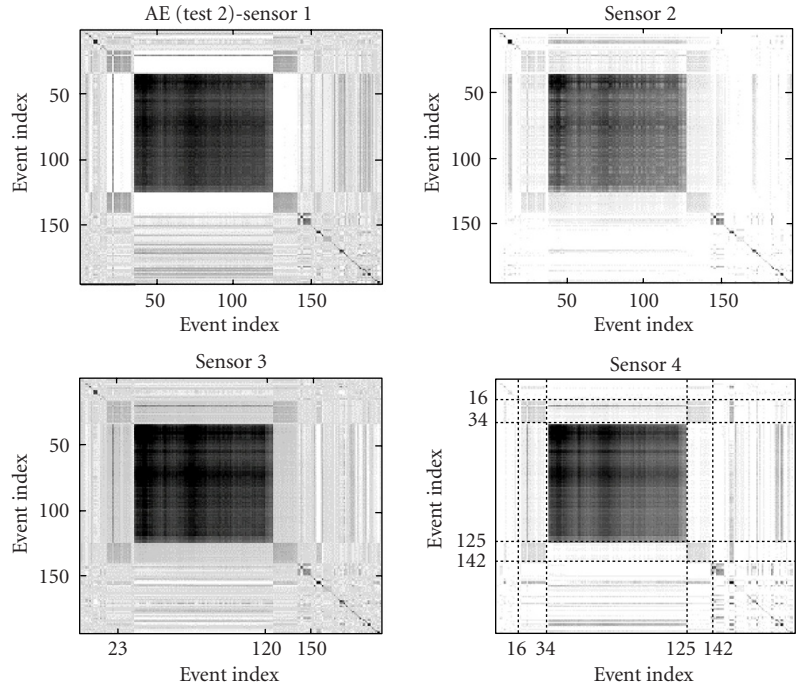

Figure 6: Cross-correlation matrix for the AE event waveforms (test 2).

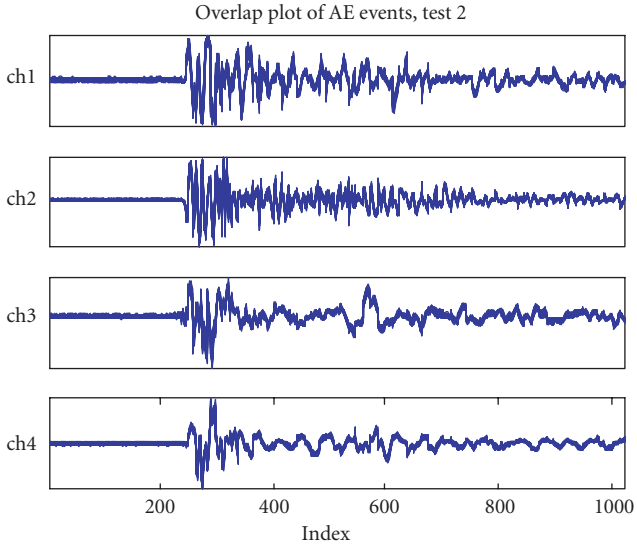

Figure 7: Overlap plot of waveforms from events 50–120 (test 2).

filtered out by an appropriate high-pass filter. Other noise observed from measurements on helicopters have indicated the existence of nonstationary broadband noise in addition to the usual white electronic noise. A linear predictor may be useful as a data-adaptive whitening filter for this noise component [12]. The prominent noise observed in this study, however, comes from the fretting or friction between gripping pads and the specimen. Events produced from these sources resemble those produced from notch crack growth, that is, they are high-frequency and contain wave propagation effects. Figures 8 and 9 show the results of PCA of the grip noise. As can be observed from the slowly decaying eigenvalues, these signals appear to be much more random than the crack signals of Figures 3 and 4.

4. CLUSTERING OF AE EVENTS FROM THE TEST DATA

In this section, a system that removes the noncrack events and applies a Kohonen network [13] to cluster the potentially crack-related AE signals is shown in Figure 10. Three techniques are employed to remove the noise events. The first used a bandpass filter 20 kHz–1 MHz to remove low frequency noise, that is, events whose ratio of energy in the frequency band to the whole energy is below a certain threshold. Second, using the first and second PCs (a larger number of PCs, for example 5, can be used if needed) we remove clusters that correspond to the grip-related signals with a radial basis function (RBF) network [14].

In the third technique, a cross-correlation is used to measure the delays between the sensors to remove events that have relatively large differential delays (more than 10 μs), that is, the grip noise. At this stage, a significant amount of noise is removed from the original test data. Next, a self-organizing map (SOM) is used to process the remaining data for separating the noise and clustering AE signals. To improve the efficiency of classification, STFT is used to retain the time-frequency characteristics of the remaining events, reducing the dimension of the data. Figure 11 shows the results of successive removal of noise from the original data.

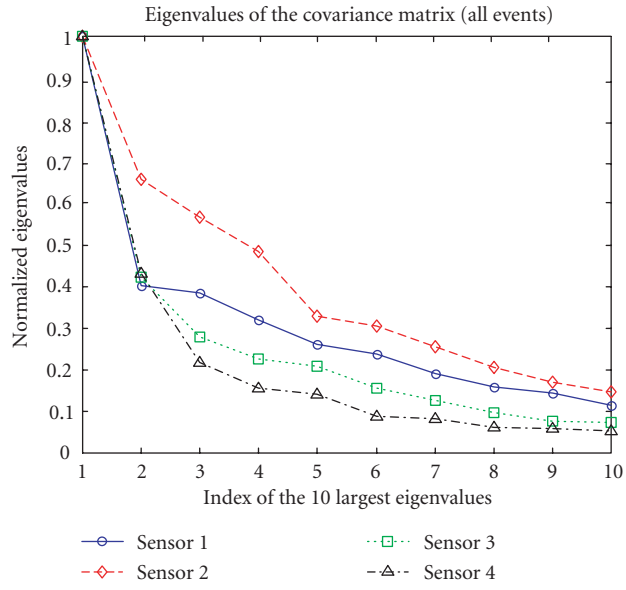

FIGURE 8: The ten largest eigenvalues of the noise covariance matrix (test 2).

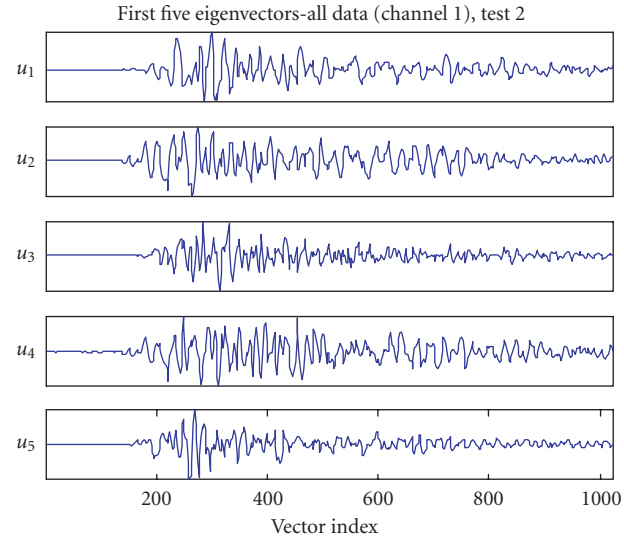

FIGURE 9: First five principal vectors for crack-generated AE signals of test 2.

4.1. Principal components of the data

In Section 3.1 we presented results of principal components analysis for AE and non-AE signals and the corresponding spaces spanned by the first few principal vectors are denoted as *signal and noise subspace*, respectively. In practice, however, the data recorded from an AE test contains both, and an algorithm has to be able to select one type or the other from the mixed data. Using this combined signal and noise data, we performed the principal component analysis. Figure 12 shows the distribution of the first two principal components associated with the output of the RBF network for each of the four sensors in test 1. It is noticed that the two principal components are mainly divided into four clusters: the cluster around the origin and three branches. Randomly choosing and plotting a signal from these four regions shows that the center cluster contains mainly AE signals, while the other three branches are noise. This is also confirmed when projecting the selected AE signals to the mixed space, and they overlap with the center cluster.

This result is not surprising. The first two PCs are heavily influenced by the intrinsic features of the grip noise since they account for more than 80% of the total events used in performing the analysis. When signals of different nature, in this case the AE signals, are projected to these two directions, it leads to a distribution of PCs around the origin, meaning no similarities exist between the AE and noise. Some overlaps of the two are due to the highly nonstationary nature of the two types of signals. We then can use the clustered PCs to remove a large number of non-AE events, either based on single sensor data or by a validation or voting rule using the PCs from all the sensors.

To separate the clusters explicitly, a simple RBF network is employed. This network, which can be implemented by associated routines in MATLAB, was found to converge faster than other neural networks for this input set of two PC components. Here the RBF classifier is a 4-node network, in which radius is the Euclidean distance between two events (first two PCs). After this stage, a significant portion of the noise data is successfully removed, and the data set is reduced by almost 50%, that is, the data is reduced from 3027 to 1506 and from 2141 to 1050, respectively, for test 1 and test 2.

4.2. Delay estimation for the multisensor data

To further reduce noise from the already halved data, a time-delay estimate is used. The estimate is based on the location of the maximum of the cross-correlation between the signals of any two sensors: for a pure delay model of propagation, two data sequences from the same source will have the maximum cross-correlation when the delay between these two data sequences is compensated. The normalized cross-correlation value above a threshold is used as the true delay. At this stage of processing, we use a relatively low threshold value (as low as 0.4) to increase the probability of capturing potential AEs. This is done at the expense of increased false alarm rate, that is, selection of noise signals. Subsequent processing is used to further discriminate between AE and noise events. Figure 13 shows the estimated differential delays between the signals received at 3 pairs of sensors. Using the delay estimation, the two test data are reduced to 500 and 645, respectively. Based on what we explained in the previous sections, events that correspond to large differential delays ($> 10\,\mu s$) are noise events.

4.3. Clustering of AE events using the Kohonen network

Some noise events still remain to be separated because of their close resemblance to the AE signals. Since no precise model for AE signals is available, a neural network-based

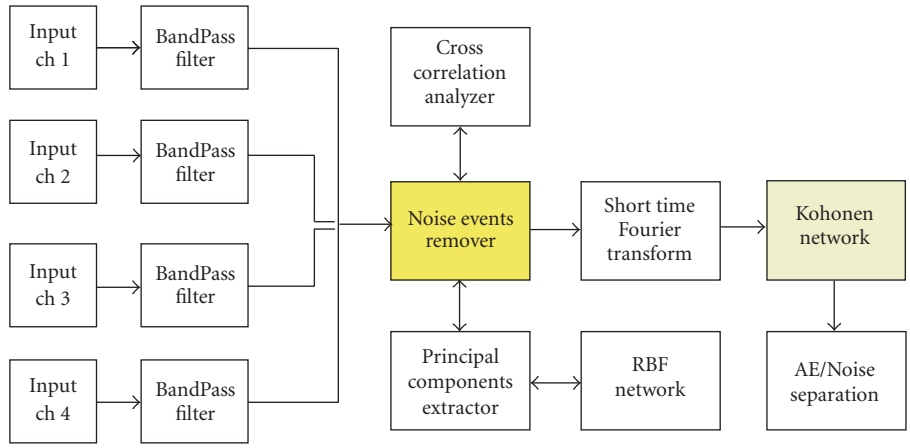

Figure 10: Proposed system for acoustic emission clustering.

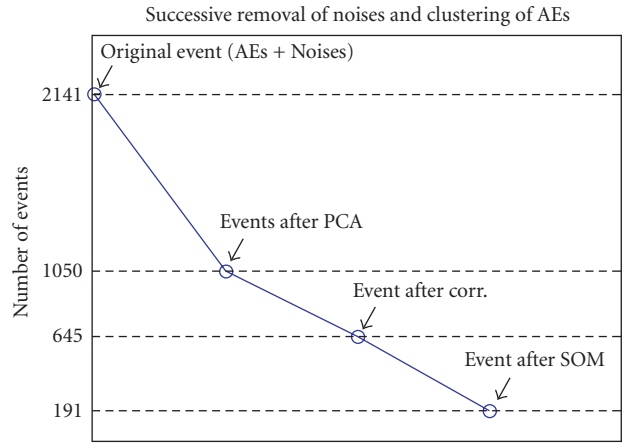

Figure 11: Results of successive removal of noise.

scheme seems to be an appropriate choice. This study uses a 4×4 Kohonen network, which yields better results than other $k \times k$ networks (e.g., 3×3 or 5×5). The network is unsupervised, that is, the network is presented with only the inputs, and samples of similar events are grouped to the same node. The training set consisted of 500 128-dimensional vectors of the STFTs of AE signals and noise, randomly chosen from the pool of one sensor. The Hamming window was used in the computation of the STFTs. However, the performance of the method was fairly invariant to the choice of the window. The test set consisted of all the remaining data from all the four sensors. Figure 14 shows which event is mapped to which neuron.

As crack-related signals have different time-frequency features compared to grip and noise-related signals, it is expected that crack-related signals to be mapped to special neurons. The results show that almost all the AE signals are mapped to neurons 2–5. Table 3 lists the AEs classified by the network. The two samples of crack-related signals detected by the Kohonen network are shown in Figure 15.

Table 3: Performance of the Kohonen network.

Test	AE events	AEs clustered	AEs missed	False alarm	Percentage of correct classification
1	385	382	5	2	98.7%
2	192	191	2	1	99.5%

5. SIGNAL SUBSPACE PROJECTION

The scheme described above assumes no a priori information about the AE signal subspace (or equivalently the noise subspace) is available. In AE testing, however, calibration of the system and repeatability of the test have to be ensured before applying the technique to engineering applications. Therefore, at least some typical AEs are available. If we are able to characterize the AE signal subspace based on the principal eigenvectors of the covariance matrix of the available AE ensemble, or equivalently the noise ensemble, the following possibilities may be explored:

(i) having identified the AE signals from one test using the developed system, we can use it as an estimate of the signal subspace for the subsequent tests;

(ii) the events prior to the possibility of any measurable crack-related events may be used to estimate the noise subspace;

(iii) the high correlation among successive events during a rapid rise in the event count may be used as an indicator of a group of potential AE events and used for estimating the AE signal subspace.

Once the signal subspace has been estimated, data from a new test can be projected onto this subspace. The norm of this projection is a measure of the closeness of the data to the signal subspace. In this case a norm of 1 is a perfect fit to the signal by the principal eigenvectors. Thus, a threshold among several sensors, if necessary, can be set for identifying the potential crack-related AE events. Similarly, noise can be classified.

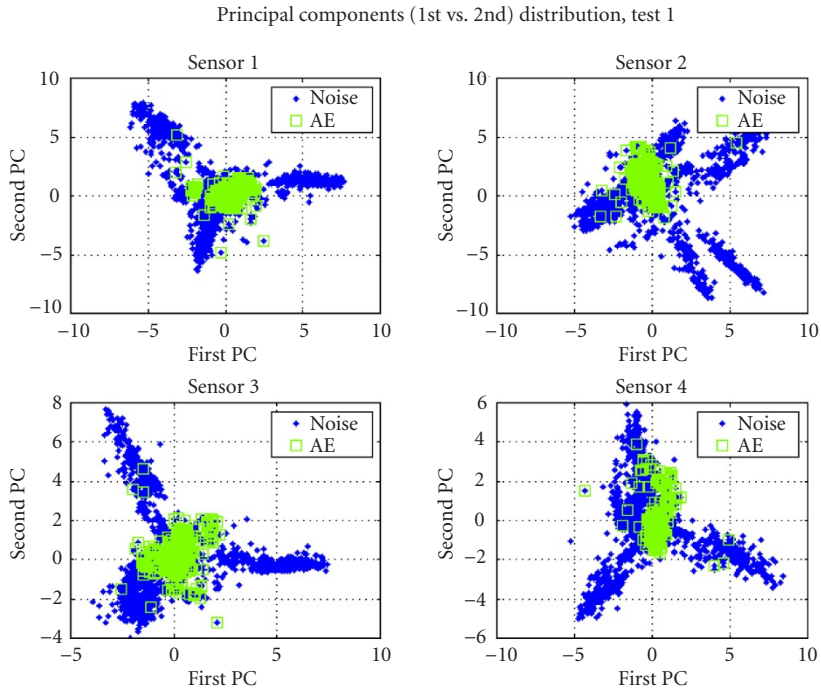

Figure 12: Second PC versus first PC for test 1 data.

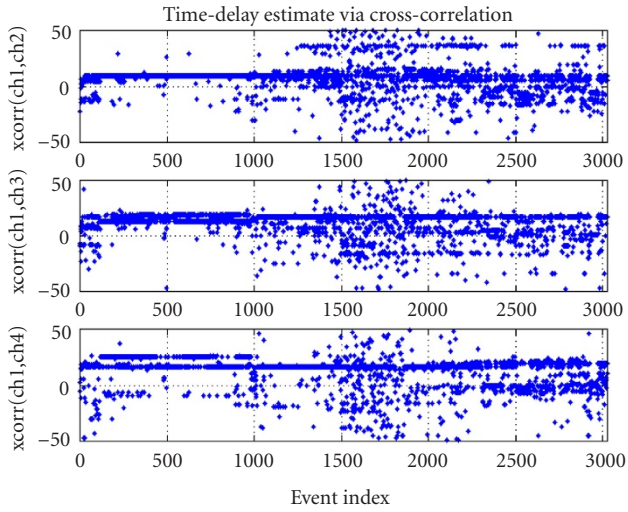

Figure 13: Delays between pairs of sensors for all 3027 events, test 1. (a) Sensors 1 and 2; (b) Sensors 1 and 3; (c) Sensors 1 and 4.

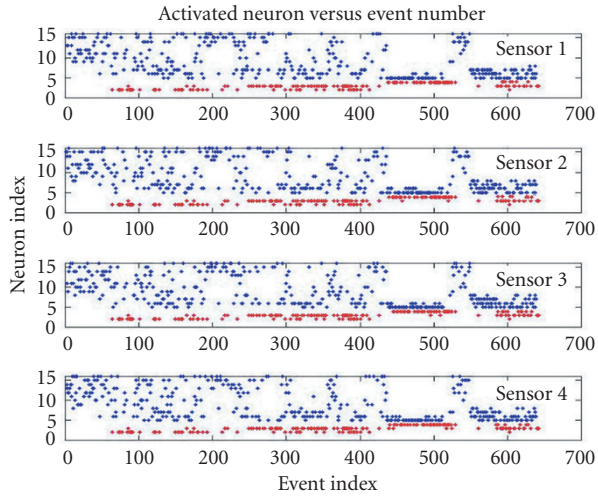

Figure 14: Output of the Kohonen network to all potentially crack-related signals.

Suppose that the recorded signal is divided into a signal component $\mathbf{x}$ and a noise component $\mathbf{n}$ that is uncorrelated with $\mathbf{x}$

$$\mathbf{s} = \mathbf{x} + \mathbf{n}. \tag{1}$$

The covariance matrix of the recorded signal

$$R_{\mathbf{ss}} = E[\mathbf{s}\mathbf{s}^T] = R_{\mathbf{xx}} + R_{\mathbf{nn}}, \tag{2}$$

with $R_{\mathbf{xx}} = E[\mathbf{x}\mathbf{x}^T]$ and $R_{\mathbf{nn}} = E[\mathbf{n}\mathbf{n}^T]$. We assume that the noise vector consists only of white noise with variance $\sigma_{\mathbf{n}}^2$, that is, $R_{\mathbf{nn}} = \sigma_{\mathbf{n}}^2\mathbf{I}$.

The M-dimensional space containing the recorded signal vectors can now be divided up into two subspaces: the *signal subspace* and the *noise subspace*. The signal subspace is the subspace spanned by the eigenvectors of the signal covariance matrix $R_{\mathbf{xx}}$; therefore,

$$\text{Signal subspace} = \text{span}\,(u_1^{\mathbf{x}}, \ldots, u_r^{\mathbf{x}}), \tag{3}$$

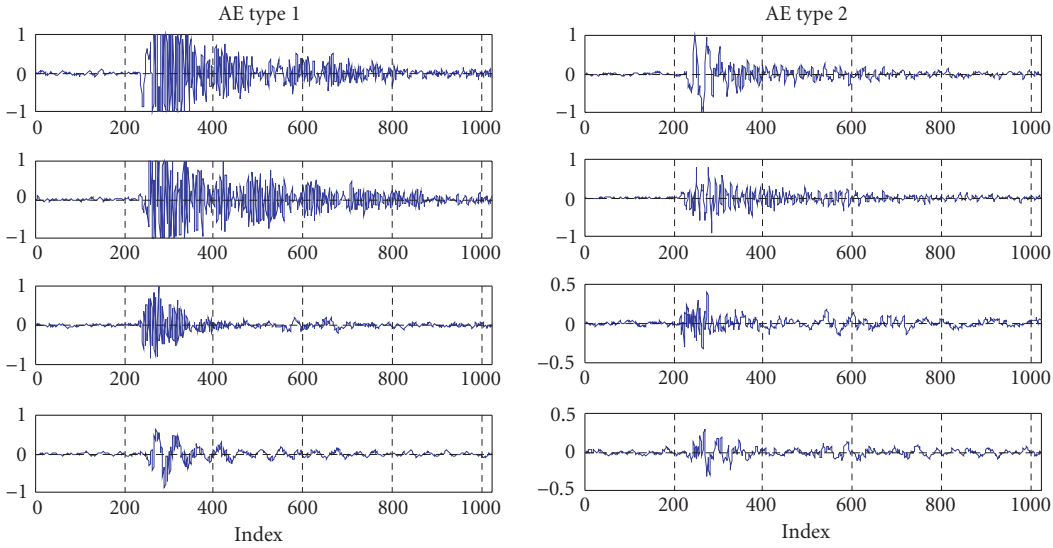

Figure 15: Samples of crack-related signals detected by the network.

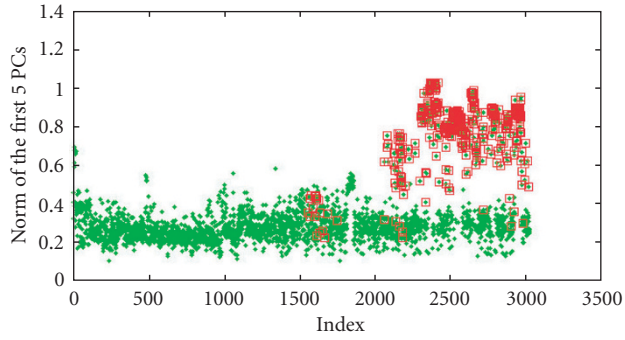

Figure 16: Norms of the projections of test 1 data onto the test 2 signals subspace.

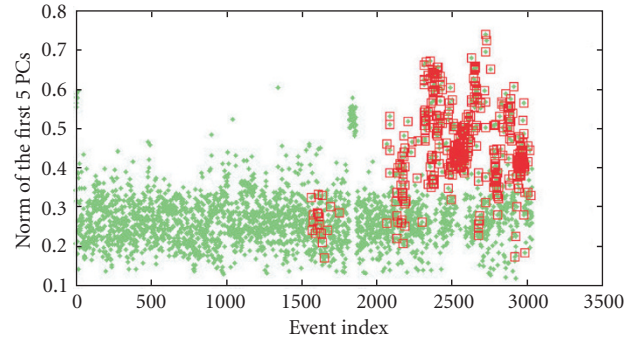

Figure 17: Norms of the projections of test 2 data onto the test 1 signal subspace.

where $u_1^{\mathbf{x}}, \ldots, u_r^{\mathbf{x}}$ are the eigenvectors corresponding to the r largest eigenvalues $\lambda_1^{\mathbf{x}}, \ldots, \lambda_r^{\mathbf{x}}$, of the signal covariance matrix. The noise subspace is the orthogonal complement of the signal subspace. The noise subspace will thus be spanned by the eigenvectors of $R_{\mathbf{ss}}$ with eigenvalues equal to $\sigma_{\mathbf{n}}^2$, and the signal subspace will be spanned by the eigenvectors of $R_{\mathbf{ss}}$ with eigenvalues strictly greater than $\sigma_{\mathbf{n}}^2$. A base of vectors spanning the signal subspace can thus be constructed by selecting the eigenvectors of $R_{\mathbf{ss}}$ with eigenvalues above the noise level $\sigma_{\mathbf{n}}^2$.

As an example, a signal subspace of dimension 5 based on the AE ensemble of test 2 is computed. Figure 16 shows the results when projecting the complete data of test 2 on the signal subspace. It is noticed that the AEs, that is, cluster with higher values of the projections, are effectively separated from the noise. Figure 17 shows the results when cross-projecting the test 1 data onto the signal subspace of test 2. The result shows 175 correct classifications, excluding 2 false alarms, out of 191 or a ratio of correct classification of 89.4% is achieved. Similarly a ratio of 91.5% is achieved when cross-projecting test 2 data onto the test 1 AE subspace. Performance of this method is illustrated in Table 4.

6. SUMMARY

This work has presented a set of algorithms for automatic clustering and separation of AE events, generated by the propagation of cracks in a metal sample, and extraneous signals with highly similar spectral components as the AEs, based on multiple features extracted from the test data. The algorithm accomplishes this by successively eliminating the non-AE noise from the record by using a combination of covariance analysis, PCA, and differential time delay estimates. In the two experimental test cases that are presented in the paper, the method correctly classifies more than 70% of the detected events as noise, before an SOM is applied to separate the AEs from the noise in the remaining data. For the two reported test cases, the final classification accuracy was around 98%. In another six test situations, with more problematic experimental conditions (such as

Table 4: Performance of the cross-projection method.

Test	Total events	AE events	AEs clustered	False alarms	Correct classifications	Percentage of correct classification
1	3027	385	353	9	344	89.4%
2	2141	192	177	2	175	91.2%

sensor problems), accuracies in the range of 85%–95% were obtained.

When prior information about the AE signal features in terms of a principal basis function is available, the results in the paper show that principal component analysis of the data can be effectively used for separating the AE signals of interest from the noise. The examples given in this study demonstrate a ratio of correct classification close to 90% using signal-subspace projections.

The parameters of the processors and networks, and data sizes that were used in the test cases of this paper were selected based on experimentation, empirical evidence and trial and error. As such, these parameters are not to be viewed as universal for any AE detection/classification, or other similar test situation. Further, these parameters were selected for the available experimental data, which resulted from a particular test of a certain metal in a specific fatigue testing machine with accompanying (grip) noise that dominated the data. Detection of AE signals accompanying crack growth in other situations will require preliminary analysis to select the processor parameters. We believe, however, that, structurally, the general approach presented, and the suite of accompanying algorithms are effective in most other similar situations.

ACKNOWLEDGMENT

This work is supported by the Office of Naval Research M-URI Program "Integrated Diagnostics" (contract number: N00014-95-1-0539).

REFERENCES

[1] C. Scala, J. McCardle, and S. Bowles, "Acoustic emission monitoring of a fatigue test of an F/A-18 bulkhead," *Journal of Acoustic Emission*, vol. 10, no. 3/4, pp. 49–60, 1992.

[2] C. Scruby, "Quantitative acoustic emission techniques," in *Research Techniques in Nondestructive Testing*, p. 141, Academic Press, London, UK, 1985.

[3] R. Barga, M. Friesel, and R. Melton, "Classification of acoustic emission waveforms for nondestructive evaluation using neural networks," in *Proc. SPIE International Symposium on Optical Engineering and Photonics in Aerospace Sensing in the Applications of Artificial Neural Networks*, vol. 1294, pp. 545–556, Orlando, Fla, USA, April 1990.

[4] G. T. Venkatesan, L. Tong, M. Kaveh, and K. Buckley, "A deterministic blind identification technique for SIMO systems of unknown model order," in *Proc. IEEE Int. Conf. Acoustics, Speech, Signal Processing*, vol. 4, pp. 1789–1792, Phoenix, Ariz, USA, March 1999.

[5] H. Sun, M. Kaveh, and A. Tewfik, "Self-organizing map neural network for transient classification in mechanical diagnostics," in *Proc. IEEE-EURASIP Workshop on Nonlinear Signal and Image Processing*, Antalia, Turkey, June 1998.

[6] V. Emamian, M. Kaveh, and A. H. Tewfik, "Robust clustering of acoustic emission signals using the Kohonen network," in *Proc. IEEE Int. Conf. Acoustics, Speech, Signal Processing*, vol. 6, pp. 3891–3894, Istanbul, Turkey, June 2000.

[7] Z. Shi, J. Jarzynski, and L. Jacobs, "Quantitative acoustic emission from localized sources in material fatigue process," in *Quantitative Nondestructive Evaluation*, Montreal, Quebec, Canada, 2000.

[8] K. Pearson, "On lines and planes of closest fit to systems of points in space," *Philosoph. Mag.*, vol. 6, no. 2, pp. 559–572, 1901.

[9] I. Jolliffe, *Principal Component Analysis*, Springer-Verlag, New York, NY, USA, 1986.

[10] I. Daniel, J. Luo, C. Sifniotopoulos, and H. Chun, "Acoustic emission monitoring of fatigue damage in metals," *Review of Progress in Quantitative Nondestructive Evaluation*, vol. 16, pp. 451–458, 1997.

[11] S. M. Ziola and M. R. Gorman, "Source location in thin plates using cross-correlation," *J. Acoust. Soc. of Amer.*, vol. 90, no. 5, pp. 2551–2556, 1991.

[12] G. T. Venkatesan, D. West, K. M. Buckley, A. Tewfik, and M. Kaveh, "Automatic fault monitoring using acoustic emissions," in *Proc. IEEE Int. Conf. Acoustics, Speech, Signal Processing*, vol. 3, pp. 1893–1896, Munich, Germany, April 1997.

[13] T. Kohonen, "The self-organizing map," *Proceedings of the IEEE*, vol. 78, no. 3, pp. 1464–1480, September 1990.

[14] S. Haykin, *Neural Networks: A Comprehensive Foundation*, Prentice-Hall, NJ, USA, 1999.

Vahid Emamian received his B.S. and M.S. degrees in electrical engineering from the Sharif University of Technology, Tehran, in 1996 and 1998, respectively, and his Ph.D. degree from the Department of Electrical and Computer Engineering at the University of Minnesota in 2003. His research interests include wireless communications, cooperative wireless networks, and digital signal processing.

Mostafa Kaveh received his B.S. and Ph.D. degrees from Purdue University in 1969 and 1974, respectively, and his M.S. degree from the University of California at Berkeley in 1970. He has been at the University of Minnesota since 1975, where he is the Centennial Professor and, since 1990, Head of the Department of Electrical and Computer Engineering. He was a design engineer at Scala Radio Corp., San Leandro, Calif, 1970, and has consulted for industry, including the MIT Lincoln Laboratory, 3M, and Honeywell. Dr. Kaveh is a fellow of the IEEE, was the recipient (with A. Barabell) of the 1986 IEEE ASSP Senior (best paper) Award, the 1988 IEEE ASSP Meritorious Service Award, an IEEE Third Millennium Medal, and the 2000 Society Award of the IEEE Signal Processing Society.

Ahmed H. Tewfik has received his B.S. degree from Cairo University, Cairo, Egypt, in 1982 and his M.S., E.E., and Sc.D. degrees from the Massachusetts Institute of Technology, Cambridge, MA, in 1984, 1985, and 1987, respectively. Dr. Tewfik is the E. F. Johnson Professor of Electronic Communications with the Department of Electrical Engineering at the University of Minnesota. From August 1997 to August 2001, he was President and CEO of Cognicity, Inc., an entertainment marketing software tools publisher that he cofounded, on partial leave of absence from the University of Minnesota. Prof. Tewfik is a Fellow of the IEEE. He was a Distinguished Lecturer of the IEEE Signal Processing Society in 1997–1999. He received the IEEE Third Millennium Award in 2000. He was invited to be a principal lecturer at the 1995 IEEE EMBS Summer School. He was awarded the E. F. Johnson Professorship of Electronic Communications in 1993. He was selected to be the first Editor-in-Chief of the IEEE Signal Processing Letters from 1993 to 1999. His current research interests are in signal processing for high performance computing I/O, multimedia and short-range high bit rate wireless communications.

Zhiqiang Shi was born in Beijing, China, in 1971. He graduated from Tsinghua University, China, in 1994, and received the M.S. degree from Tennessee Technological University in 1996 and the Ph.D. degree from Georgia Institute of Technology in 2001, all in mechanical engineering. Since 2001, he has joined Manufacturing Technology and Engineering, Corning Incorporated, and has been working on nondestructive testing for industrial applications. Dr. Shi is a member of the Acoustical Society of America and the American Society for Nondestructive Testing.

Laurence J. Jacobs received his B.S. in Civil Engineering, Lafayette College, Easton, Pa., USA, 1979 and his M.S. in Civil Engineering (Structures), Polytechnic Institute of New York, Brooklyn, NY, USA, in 1981 and his Ph.D. in Engineering Mechanics from Columbia University, New York, NY in 1987. He joined the School of Civil and Environmental Engineering, Georgia Institute of Technology, Atlanta, GA, USA, as an Assistant Professor in 1988, and became a full Professor in 2000. Professor Jacobs' research focuses on the development of quantitative methodologies for the nondestructive evaluation of structural materials.

Jacek Jarzynski received his B.S. from Imperial College, London, in 1957 and his Ph.D. from Imperial College, London in 1961. He began his work at Georgia Institute of Technology in winter, 1986 as a Professor, and retired in May 2001. He was Chief Scientist in the Acoustics Division at the Physical Acoustics Branch of the Naval Research Laboratory. Dr. Jarzynski has been involved in research in various areas of acoustics, ranging from ultrasonics to underwater acoustics, and some areas of optics. His research also includes the development of optical, noncontact techniques for measurements of vibrations, measurements of acoustical and elastic properties of composite materials, ultrasonic transmission and acoustic emission measurements to detect fatigue failure in metals, and development of fiber optic acoustic and ultrasonic sensors. He was a physical acoustics committee member and fellow of Acoustical Society of America from 1994 to 1997. He has received Best Publication Awards from Naval Research Laboratory Acoustics Division in 1978, 1980, 1981, and 1985, as well as Best Publication on Fiber Optic Sensors Award from National Aeronautics and Space Administration in 1987.